

Field gradient calculation of HTS double-pancake coils considering the slanted turns and the splice

Geonwoo Baek^a, Jinsub Kim^a, Woo Seung Lee^b, Seunghyun Song^a, Onyou Lee^c, Hyoungku Kang^c, and Tae Kuk Ko^{*a}

^a Yonsei University, Seoul, Korea

^b JH ENGINEERING CO., LTD., Gunpo, Korea

^c Korea National University of Transportation, Chungju, Korea

(Received 8 February 2017; revised or reviewed 15 March 2017; accepted 16 March 2017)

Abstract

To obtain Nuclear Magnetic Resonance (NMR) measurement of membrane protein, an NMR magnet is required to generate high intensity, homogeneity, and stability of field. A High-Temperature Superconducting (HTS) magnet is a promising alternative to a conventional Low-Temperature Superconducting (LTS) NMR magnet for high field, current density, and stability margin. Conventionally, an HTS coil has been wound by several winding techniques such as Single-Pancake (SP), Double-Pancake (DP), and layer-wound. The DP winding technique has been frequently used for a large magnet because long HTS wire is generally difficult to manufacture, and maintenance of magnet is convenient. However, magnetic field generated by the slanted turns and the splice leads to field inhomogeneity in Diameter of Spherical Volume (DSV). The field inhomogeneity degrades performance of NMR spectrometer and thus effect of the slanted turns and the splice should be analyzed. In this paper, field gradient of HTS double-pancake coils considering the slanted turns and the splice was calculated using Biot-Savart law and numerical integration. The calculation results showed that magnetic field produced by the slanted turns and the splice caused significant inhomogeneity of field.

Keywords: double-pancake coils, field gradient, Romberg integration, slanted turns, splice

1. INTRODUCTION

Since high-temperature oxide superconductivity material was discovered in 1989 [1], a lot of research has been conducted to apply High-Temperature Superconducting (HTS) coils to Nuclear Magnetic Resonance (NMR) magnets because of limit in critical fields of Low-Temperature Superconducting (LTS) coils in high field region for about 23 T [2]. HTS coils are indispensable for high field NMR magnets.

NMR magnets require field homogeneity of below 1 Part Per Billion (ppb) in 3 cm Diameter of Spherical Volume (DSV) to analyze structure of membrane protein such as aquaporin [2], and fabrication of coils that generate a magnetic field distribution with high uniformity is related to design of coil shape [3]. Minimization of objective functions such as ppb in DSV and axial harmonics is one of effective techniques that are designed to attain field distribution with high uniformity [3].

However the optimization method based on field calculation of ideal solenoid causes inaccurate field distribution. Magnetic field calculation for air-core solenoids can be easily found in [4]. Practically, an HTS magnet has been frequently wound by double-pancake winding method. Thus, the slanted turns and the splice between adjacent layers in Double-Pancake Coils (DPCs) are unavoidable as shown in Fig. 1. These additional turns

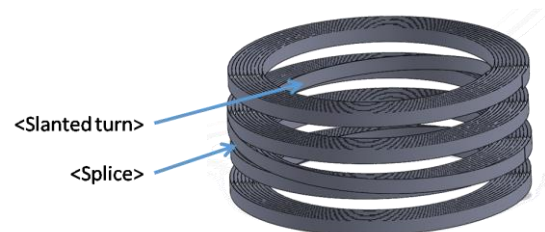


Fig. 1. The slanted turns and the splice of two DPCs.

may generate undesirable field gradient in manufacturing of an HTS magnet composed of DPCs. Therefore, the effect of the slanted turns and the splice in an HTS magnet should be analyzed.

In this paper, magnetic flux density calculation program for these additional turns using Biot-Savart law and numerical integration was developed because Finite Element Method (FEM) is not able to provide proper accuracy (ppb) [5]. In addition, field gradient of HTS DPCs considering the slanted turns and the splice was calculated. The calculation results showed that magnetic field produced by the slanted turns and the splice caused significant inhomogeneity of field.

2. BASIC FORMULA

2.1. Biot-Savart law

* Corresponding author: tkko@yonsei.ac.kr

Magnetic field intensity generated by steady current is given as

$$\vec{B}(\vec{r}') = \frac{\mu_0 I}{4\pi} \int \frac{d\vec{l} \times \hat{\eta}}{|\vec{\eta}|^2} \quad (1)$$

where \vec{r}' is the position vector indicating a target point, $d\vec{l}$ is the infinitesimal displacement vector of conductor carrying current, I, μ_0 is the permeability of free space, and $\vec{\eta}$ is the displacement vector from source to a target point [6].

2.2. Modeling with thin half elliptical wire

To apply (1) to the slanted turns and the splice of DPCs, its mathematically defined shape should be defined. Firstly, to simplify the problem, it is assumed that the slanted turns and the splice of DPCs are infinitely thin. Secondly, it is assumed that the slanted turns and the splice of DPCs are wound spirally on the bobbin. However, if an HTS tape is bent, it will return to its original shape by elastic force because the substrate of an HTS tape is a metal. Thus, it is reasonable to assume the slanted turns and the splice of DPCs are wound diagonally on the bobbin. Finally, it is assumed that the slanted turns and the splice of DPCs have half turn.

The circumference of the circular cylinder cut diagonally due to the geometric characteristics of the circular cylinder is an ellipse shape. Therefore, magnetic fields from the slanted turns and the splice of DPCs are same as that from thin half elliptical wire. According to definition of ellipse, all the points on the elliptical wire for which major and minor axes are $2R$ and $2r$ can be represented by circles of radius R and r as shown in Fig. 2. Therefore, magnetic field generated by thin half elliptical wire carrying current, I , can be expressed as follows.

$$\vec{B}_x(\vec{r}') = \frac{\mu_0 I}{4\pi} \cdot \int_0^\pi \frac{(zr \cos \varphi) \hat{i}}{D} d\varphi \quad (2)$$

$$\vec{B}_y(\vec{r}') = \frac{\mu_0 I}{4\pi} \cdot \int_0^\pi \frac{(zR \sin \varphi) \hat{j}}{D} d\varphi \quad (3)$$

$$\vec{B}_z(\vec{r}') = \frac{\mu_0 I}{4\pi} \cdot \int_0^\pi \frac{(-yR \sin \varphi - xr \cos \varphi + rR) \hat{k}}{D} d\varphi \quad (4)$$

$$D = (x^2 + y^2 + z^2 - 2xR \cos \varphi - 2yr \sin \varphi + R^2 \cos^2 \varphi + r^2 \sin^2 \varphi)^{3/2}$$

2.3. Modeling with thick half elliptical wire

Equations (2)-(4) have been applied to the thin model. In practical, the slanted turns and the splice of DPCs are not thin, but thick. Thus, the triple integral is needed. The components of magnetic field generated by thick half elliptical wire, the slanted turn of DPC, with current density, J , are given by

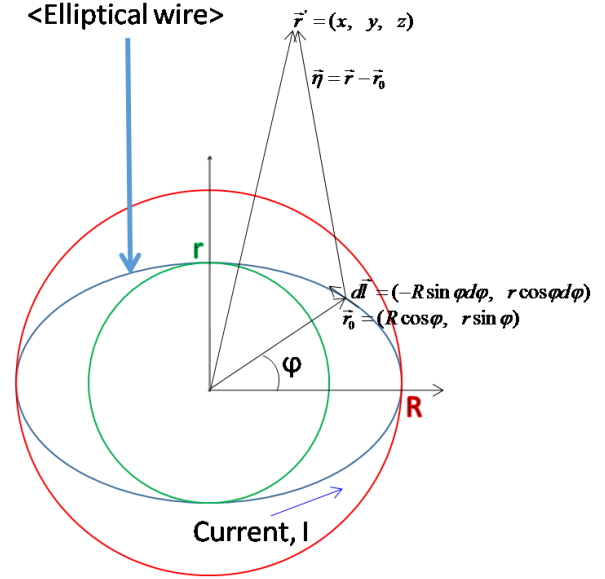


Fig. 2. Elliptical wire carrying current, I , in Cartesian coordinate system.

$$\vec{B}_x(\vec{r}') = \frac{\mu_0 J}{4\pi} \cdot \int_{w_1}^{w_2} \int_0^t \int_0^{2\pi} \frac{(z-h)(r+\rho)(\cos \varphi) \hat{i}}{D} d\varphi d\rho dh \quad (5)$$

$$\vec{B}_y(\vec{r}') = \frac{\mu_0 J}{4\pi} \cdot \int_{w_1}^{w_2} \int_0^t \int_0^{2\pi} \frac{(z-h)(R+\rho)(\sin \varphi) \hat{j}}{D} d\varphi d\rho dh \quad (6)$$

$$\vec{B}_z(\vec{r}') = \frac{\mu_0 J}{4\pi} \cdot \int_{w_1}^{w_2} \int_0^t \int_0^{2\pi} \frac{N \hat{k}}{D} d\varphi d\rho dh \quad (7)$$

$$N = \{-y(R+\rho) \sin \varphi - (x+|h-w_2| \tan \text{tilt})(r+\rho) \times \cos \varphi + (r+\rho)(R+\rho)\}$$

$$D = \{(x+|h-w_2| \tan \text{tilt})^2 + y^2 + (z-h)^2 - 2(x+|h-w_2| \tan \text{tilt})(R+\rho) \cos \varphi - 2y(r+\rho) \times \sin \varphi + (R+\rho)^2 \cos^2 \varphi + (r+\rho)^2 \sin^2 \varphi\}^{3/2}$$

$$R = \frac{\sqrt{(s+t)^2 + (2a_1)^2}}{2}, \quad r = a_1, \quad \text{tilt} = \arctan \frac{s+t}{2a_1}$$

where ρ is the thickness variable of the slanted turn, t is the thickness of the slanted turn, h is the width variable of the slanted turn, w_2-w_1 is the width of the slanted turn, s is the thickness of spacer, a_1 is the inner radius of DPC, and tilt is the angle of inclination. If a_1 which is the inner radius of DPC is replaced by a_2 which is the outer radius of DPC, (5)-(7) represent magnetic field intensity due to the splice of DPCs. Finally, rotational transform of magnetic field from (5)-(7) should be required because the slanted turns and the splice of DPCs are inclined.

3. NUMERICAL INTEGRATION

3.1. Romberg integration algorithm

Because it is very difficult to solve (5)-(7) analytically, a numerical integration technique must be introduced.

Romberg integration algorithm which is widely known as a suitable algorithm for computer program was employed [7]. The Romberg integration algorithm method uses trapezoidal rule and Richardson's extrapolation, which uses two approximations to compute third refined approximation, to improve approximation more accurately. Formula of Romberg integration algorithm can be expressed as follows.

$$I_{j,k} \cong \frac{4^{k-1}I_{j+1,k-1} - I_{j,k-1}}{4^{k-1} - 1} \quad (8)$$

where $I_{j+1,k-1}$ and $I_{j,k-1}$ are two estimates of trapezoidal rule, and more improved $I_{j,k}$ can be obtained by applying weighted average to a more accurate approximation, $I_{j+1,k-1}$.

Romberg integration algorithm implements iteratively until the percent relative error, ε_a , of approximate value becomes within the acceptable level, ε_s . It is called stopping or termination criterion. The error is related to the number of significant figures [8].

$$|\varepsilon_a| = \left| \frac{I_{1,k} - I_{2,k-1}}{I_{1,k}} \right| \times 100\% \leq \varepsilon_s = (0.5 \times 10^{2-n})\% \quad (9)$$

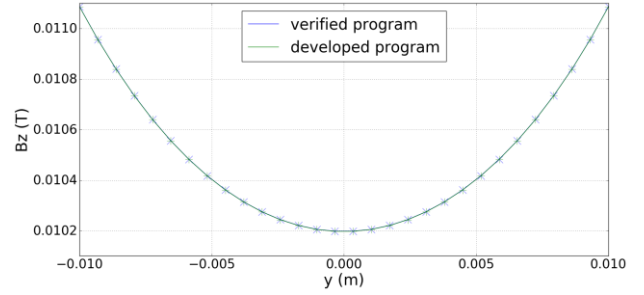
Magnetic field having an accuracy of ppb can be obtained by selecting the appropriate stopping criterion. As the accuracy of magnetic field become higher, the computing time will become longer. Computing time of the suggested analytical method with different stopping criterion is as follows. Computing time is 2.54 s if stopping criterion is $5 \times 10^{-5}\%$, computing time is 19.9 s if stopping criterion is $5 \times 10^{-9}\%$.

3.2. Verification of the developed program

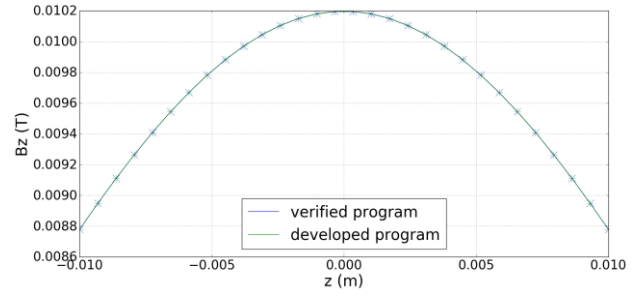
A program calculating magnetic field of the slated turns and the splice of DPCs at a point of interest was developed using Python computer program and numerical integration of (5)-(7). Before calculating field gradient of DPCs considering the slanted turns and the splice, the developed program should be verified.

If the thickness of spacer is zero and the azimuthal range is modified from 0 to 2π in triple integral of thick half elliptical wire model, the shape of the conductor is same as the ideal solenoid. The magnetic field for the ideal solenoid can be easily obtained using the program as in [4]. However, employing the analytical solution of the thin solenoid [9] can improve the speed and the accuracy of program. Python program on the basis of the analytical solution of the thin solenoid was also developed. Thus, the reliability of a program calculating magnetic field of the slated turns and the splice of DPCs can be indirectly verified by using a magnetic field calculation program for the ideal solenoid.

Axial field at y- and z-axes in the ideal solenoid, which has the inner radius 30 mm, the outer radius 31.5 mm, the height 4 mm, operating current 50 A, and 10 turns, was obtained using the developed programs as shown in Fig. 3. It could be seen that the axial field at y- and z-axes in the



(a) y-axis



(b) z-axis

Fig. 3. Axial field at (a) y-axis and (b) z-axis in the ideal solenoid obtained using the developed programs.

TABLE I
SPECIFICATIONS OF DPCS.

Parameter	Value
Tape width	4 mm
Tape thickness	0.15 mm
Inner radius	30 mm
Outer radius	31.5 mm
Layers	4
Turns per layer	10 turns
Spacer thickness	1 mm
Operating current	50 A

ideal solenoid is almost exactly the same. Thus, a program calculating magnetic field of the slated turns and the splice of DPCs can be reliable.

4. FIELD GRADIENT CALCULATION

4.1. Spherical harmonics expansion

In region containing no current source, axial field at a target point in spherical coordinate system is expressed as

$$B_z(r, \theta, \varphi) = \sum_{n=0}^{\infty} \sum_{m=0}^n r^n (n+m+1) P_n^m(\cos \theta) \times (A_n^m \cos m\varphi + B_n^m \sin m\varphi) \quad (10)$$

where (r, π, ϕ) is a target point in spherical coordinate system, n and m are integers, P is the associated Legendre polynomials, and A and B are constants determined by the shape of the coil [10].

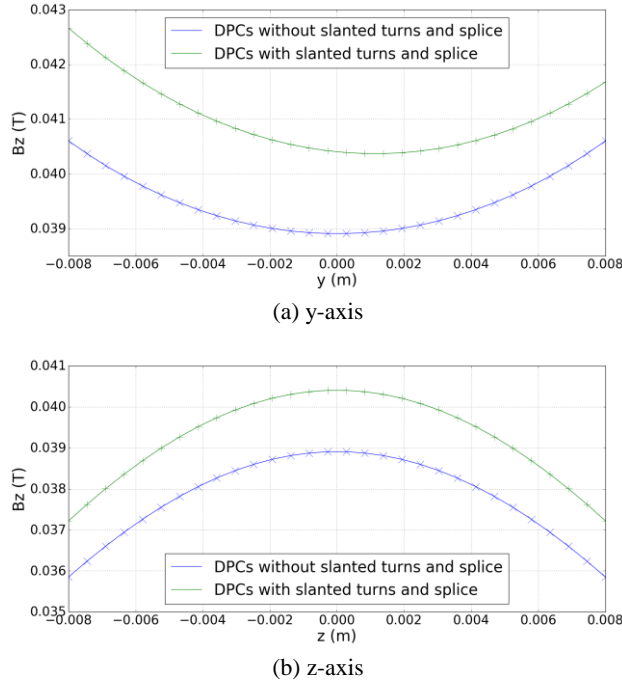


Fig. 4. Axial field of DPCs with and without the slanted turns and the splice at (a) y-axis and (b) z-axis.

TABLE II

FIELD GRADIENT OF DPCs WITH AND WITHOUT THE SLANTED TURNS AND THE SPLICE.

Parameter	DPCs without the slanted turns and the splice	DPCs with the slanted turns and the splice
B_0 [T]	3.89×10^{-2}	4.04×10^{-2}
Z [T/m]	1.67×10^{-5}	2.81×10^{-5}
X [T/m]	-3.86×10^{-7}	2.64×10^{-5}
Y [T/m]	6.59×10^{-7}	-2.02×10^{-2}
Z^2 [T/m ²]	-1.69×10	-1.76×10
ZX [T/m ²]	7.67×10^{-5}	3.42×10^{-3}
ZY [T/m ²]	1.25×10^{-3}	1.33×10^{-3}
$X^2 - Y^2$ [T/m ²]	2.00×10^{-5}	6.90×10^{-6}
XY [T/m ²]	3.56×10^{-7}	-2.88×10^{-4}

A and B is also called spherical harmonics coefficients. From the data of the magnetic field measured at various points, spherical harmonics coefficients can be determined by using least square solution [3]. Mapping is usually done by using spherical or cylindrical helix because mapping points should become independent. If mapping points are not dependent, singular value decomposition can be employed. From this, field gradient of magnet in DSV is calculated.

4.2. Simulation results

Fig. 1. and Table I shows schematics and specifications of DPCs for simulation of field gradient, respectively.

The axial field of DPCs with the slanted turns and the splice is larger than that of DPCs without the slanted turns and the splice at z-axis as shown in Fig. 4(b). This is a

natural consequent because the slanted turns and the splice generate magnetic field. However, in y-axis, the slanted turns and splice make axial field not only different in magnitude but also asymmetric as shown in Fig. 4(a). Radial field gradients are generated because of the shape characteristics of the slanted turns and splice of DPCs. Table II shows field gradients of DPCs with and without the slanted turns and the splice. To calculate field gradient, spherical harmonics were expanded to 4th order and spherical helix mapping is used. It is natural that central field of DPCs considering the slanted turns and the splice increases because the additional turns is considered. Difference of axial field gradients (Z , Z^2) between DPCs with and without the slanted turns and splice is slight. On the other hand radial field gradients (X , Y , ZX , XY) of DPCs with the slanted turns and the splice are varied from tens to hundred thousands of magnitude compared to those of DPCs without the slanted turns and the splice. This is because of the inclined half turn. Consequently, the slanted turns and the splice are significant to field error in the case of the magnet used here. In NMR-class HTS magnet consists of double-pancake, the slanted turns could be critical for the field homogeneity because the number of the slanted turns and the operating current increase.

5. CONCLUSIONS

Expression for B field of the slanted turns and the splice of DPCs was derived. To solve the triple integral, Romberg integration algorithm was employed. A program calculating magnetic field of the slanted turns and the splice of DPCs at a point of interest was developed using Python computer program and numerical integration. By calculating and comparing the field gradients of DPCs with and without the slanted turns and the splice, fact that the slanted turns and the splice of DPCs have an effect on field gradients in DSV was confirmed. Especially, radial field gradients were generated. Therefore, when designing homogeneous magnet, the slanted turns and the splice of DPCs should be considered. The developed program can be useful in NMR design to achieve high homogeneity. In addition, the reliability of the developed program was indirectly verified using a magnetic field calculation program developed on the basis of the analytical solution of the thin solenoid.

ACKNOWLEDGMENT

This work was supported in part by National R&D Program through the National Research Foundation of Korea (NRF) funded by the Ministry of Science, ICT and Future Planning, and by ‘‘Human Resources Program in Energy Technology’’ of Korea Institute of Energy Technology Evaluation and Planning (KETEP), granted financial resource from the Ministry of Trade, Industry & Energy, Republic of Korea. (Nos. NRF-2015M1A7A1A02050725 and 20164030201100)

REFERENCES

- [1] Thomas P. Sheahan, *Introduction to High-Temperature Superconductivity*, Kluwer Academic Publishers, Dordrecht, 2002.
- [2] Hideaki Maeda and Yoshinori Yanagisawa, "Recent Developments in High-Temperature Superconducting Magnet Technology (Review)," *IEEE Trans. Appl. Supercond.*, vol. 24, no. 3, pp. 4602412, 2014.
- [3] H. B. Jin, "A Study on the Design and Fabrication of Actively Shielded Superconducting MRI Magnet," PhD thesis, Sungkyunkwan University, Suwon, 1996.
- [4] Li Huang and Sangjin Lee, "Development of a magnetic field calculation program for air-core solenoids which can control the precision of a magnetic field," *Progress in Superconductivity and Cryogenics*, vol. 16, no. 4, pp. 53-56, 2014.
- [5] Antoine Chance and Guy Aubert, "Relations Between the Winding Errors of the Double Pancakes and the Spherical Harmonics Expansion of the Field," *IEEE Trans. Appl. Supercond.*, vol. 19, no.6, pp. 3795-3804, 2009.
- [6] David J. Griffiths, *Introduction to Electrodynamics*, Prentice Hall, New Jersey, 2006.
- [7] Steven C. Chapra and Raymond P. Canale, *Numerical Methods for Engineers*, McGraw-Hill, New York, 2010.
- [8] I. B. Scarborough, *Numerical Mathematical Analysis*, Johns Hopkins Press, Baltimore, 1966.
- [9] Edmund E. Callaghan and Stephen H. Maslen, "The magnetic field of a finite solenoid," *National Aeronautics and Space Administration Washington*, pp. 3, 1960.
- [10] R. Turner, "Gradient Coil Design: A Review of Methods," *Magnetic Resonance Imaging*, pp. 903-920, 1993.